Photonic generation of power-efficient FCC-compliant ultra-wideband waveforms using semiconductor optical amplifier (SOA): theoretical analysis and experiment verification*

Dong Jian-Ji(董建绩)†, Luo Bo-Wen(罗博文), Huang De-Xiu(黄德修), and Zhang Xin-Liang(张新亮)

Wuhan National Laboratory for Optoelectronics, School of Optoelectronic Science and Engineering, Huazhong University of Science and Technology, Wuhan 430074, *China*

(Received 12 May 2011; revised manuscript received 12 July 2011)

We theoretically design a power-efficient ultra-wideband pulse generator by combining three monocycle pulses with different weights. We also experimentally demonstrate a feasible scheme to generate such power-efficient ultra-wideband waveforms using cross-phase modulation in a single semiconductor optical amplifier. The designed ultra-wideband pulse fully satisfies the requirements for the spectral mask specified by the Federal Communications Commission with high power efficiency. In the experiment, a power-efficient ultra-wideband waveform with a pulse duration of 310 ps is achieved, and the power efficiency is greatly improved compared with that of a single monocycle pulse or a mixture of two monocycles.

Keywords: semiconductor optical amplifier, ultra-wideband generation, radio frequency photonics

PACS: 32.30.Bv, 84.40.–x, 42.79.Sz **DOI:** 10.1088/1674-1056/21/4/043201

1. Introduction

Ultra-wideband (UWB) technology has aroused great interest in the past few years for its advantages of high data rate, low power consumption, and immunity to multipath fading in short-range wireless communications.[1] Limited by the low emission power lower than −41.3 dBm/MHz specified by Federal Communications Commissions (FCC),[2] the UWB signal can transmit only up to tens of meters in an indoor environment. However, due to the obstruction for the wireless UWB signals to penetrate walls, a fiber-based in-home infrastructure is required for the distribution of the UWB signals for indoor use.[3] Hence the generation and the processing of UWB pulses in the optical domain have attracted much attention recently, since all-optical signal processing can be easily incorporated into UWB-over-fiber communication networks.[4−6] Consequently the UWB signals can be transmitted hundreds of kilometers rather than several meters of indoor communication over the optical fiber.[7] Photonic generation of UWB signals by different approaches has been reported so far such as by using semiconductor optical amplifiers (SOAs),[8−10] semiconductor lasers,[11,12] standard single mode fibers,[13] and fiber optical parametric amplifiers,[14] and so forth. SOA is one of the most promising candidates to generate UWB signals since it has ultrafast dynamic response in optical signal processing.[15,16]

Another critical issue is the choice of UWB pulse types. Gaussian monocycle and doublet pulses are considered as promising candidates for UWB communications due to better bit-error rates and multipath resilience among different impulse signals. However, these widely used pulses are not fully suited for the FCC mask. Recently, photonic arbitrary waveform generation techniques have emerged, and they can design special UWB waveforms to meet the FCC definition.[17,18] Abtahi *et al.*[19] presented the generation of arbitrary waveform by using thermally-controlled apodized fiber Bragg grating (FBG) and experimentally demonstrated for the first time power-efficient FCC-compliant UWB waveforms, which were obtained by combining monocycle pulses with differ-

*Project supported by the National Basic Research Program of China (Grant No. 2011CB301704), the National Natural Science Foundation of China (Grant No. 60901006), and the Fundamental Research Funds for the Central Universities of China (Grant No. 2010QN033).

†Corresponding author. E-mail: jjdong@mail.hust.edu.cn

© 2012 Chinese Physical Society and IOP Publishing Ltd

ent time delays and different weights.[20] A power-efficient UWB waveform was achieved by combining at least 7 monocycle units without power attenuation. Besides, Abraha *et al.*[21] proposed a power-efficient UWB pulse based on the combination of two monocycle pulses with different pulse widths, and FCC-compliant UWB pulses were also designed with the combination of two asymmetric monocycles.[22,23] Although the radio frequency (RF) power efficiency was greatly improved, the obtained RF spectrum still needs power attenuation to satisfy the requirements for the FCC mask.

In this paper, we design power-efficient UWB waveforms by combining a serial of weighted monocycle pulses with appropriate time delays. It is proved that only three monocycle units ($L = 3$, number of monocycles) are required to meet the FCC's criterion without power attenuation. This inference is crucial to the design of the UWB waveforms by simple configurations. Furthermore, a proof-of-concept experiment has been demonstrated to prove the feasibility of our scheme. The RF spectra of $L = 3$, $L = 2$, and $L = 1$ are compared. It is shown that the power efficiency of $L = 3$ is greatly improved compared with that of $L = 2$ and $L = 1$, respectively.

2. Design criterion of FCC-compliant UWB waveform

As we know, the RF power spectra emitted by UWB transmit antennas must be subject to the FCC spectral mask. Ideally, the FCC spectral mask can be satisfied for any pulse shape by simply reducing the average radiation power. However, received UWB signals are highly power limited, and a reduction of transmitted power will greatly degrade the performance. Since the RF spectra of Gaussian monocycle, doublet, and triplet pulses do not fully match the FCC mask, a UWB waveform optimization is very necessary. And the optimized UWB pulse should be designed to maximize the power efficiency without attenuating the signal power. We follow the approach in Ref. [20], designing the UWB pulse with the summation of a serial of Gaussian monocycle pulses, which is expressed as

$$p(t) = \sum_{n=0}^{L} \omega[n] \cdot g(t - nT_0), \tag{1}$$

where $\omega[n]$ is the weight factor for each monocycle pulse, L is monocycle number, T_0 is pulse interval, $g(t) = At\exp[-\frac{1}{2}(t/T_1)^2]$ is the monocycle pulse, i.e. the first derivative of Gaussian pulse, $T_1 = T_{\mathrm{FWHM}}/(2\sqrt{2\ln 2})$, with T_{FWHM} being the pulse width of the Gaussian pulse, and A is a scaling constant.

To optimize the UWB waveform, there are two criteria. First, the generated RF spectrum must be covered by the FCC mask without power attenuation. Second, the power efficiency must be as high as possible. The power efficiency ψ is defined as the average spectral power normalized by the total admissible power of the FCC mask, which is expressed by

$$\psi = \int_0^{\omega_{\max}} P(\omega)\,\mathrm{d}\omega \Big/ \int_0^{\omega_{\max}} S_{\mathrm{FCC}}(\omega)\,\mathrm{d}\omega, \tag{2}$$

where $S_{\mathrm{FCC}}(\omega)$ is the FCC spectral mask, $P(\omega)$ denotes the Fourier transform of $p(t)$, and $F_{\max} = \omega_{\max}/2\pi$ is the terminal frequency of interest, which is 15 GHz in our design. It is known that the RF spectrum of a single monocycle pulse ($L = 1$) does not match the FCC mask. When $L = 2$ and 3, the RF spectra are optimized by adjusting the Gaussian pulse width T_{FWHM} and pulse delay T_0. Defining that an overflow parameter $F = -1$ if $\min\{S_{\mathrm{FCC}}(\omega) - P(\omega)\} < 0$, or else $F = 0$. Hence $F = -1$ means that the RF spectrum overflows; otherwise it is FCC-compliant. Figure 1 shows the distribution of overflow parameter F as T_{FWHM} and T_0 vary. Regarding $L = 2$, there is no FCC-compliant spectrum available. For $L = 3$, the weight factors are 1, −1.5, and 1, and there

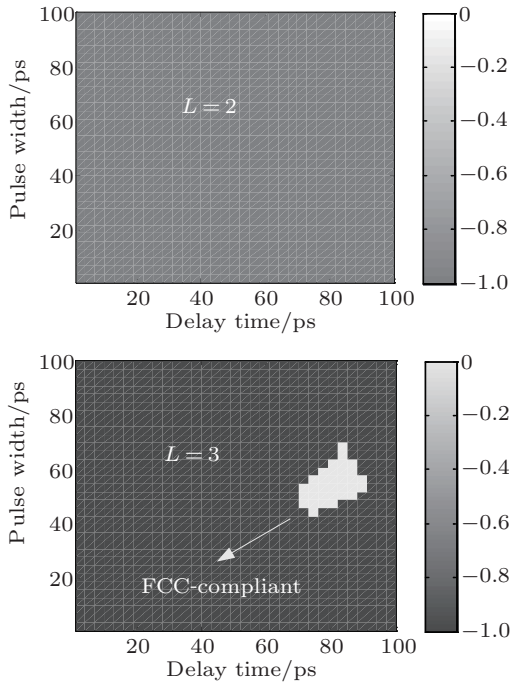


Fig. 1. Overflow parameter F distributions for $L = 2$ and 3. It is proved that an FCC-compliant UWB pulse is achievable when $L = 3$, but not when $L = 2$.

is a small white plot showing an FCC-compliant spectrum, which means that at least three monocycles are required to generate an FCC-compliant UWB pulse without power attenuation. Note that in Ref. [20], an FCC-compliant UWB waveform is achieved when $L = 7$, whereas we have proved $L = 3$ is the minimum number, which makes the design much simpler.

The optimal designed pulses for $L = 1$, 2, and 3 are plotted in Fig. 2(a). We set $T_0 = 75$ ps, and $T_{\mathrm{FWHM}} = 50$ ps. The corresponding normalized spectra of the pulses are shown in Fig. 2(b). When $L = 1$ or 2, the spectrum of the designed pulse overflows the FCC mask. By attenuating the spectral power to respect the FCC mask, the calculated power efficiencies are 0.32% and 1.38% for $L = 1$ and 2 respectively. When $L = 3$, the spectrum of the pulse complies with the FCC mask well, and the power efficiency is 45.66% without power attenuation. Although the power efficiency increases with the increase of number L, a larger number of monocycles make it difficult and complex to generate a stable UWB pulse. We also calculate the power efficiencies of doublet and triplet pulses, which are very low since the normalized RF spectrum inevitably overflows. This validates that the derivatives of Gaussian pulses do not fully satisfy the FCC mask.

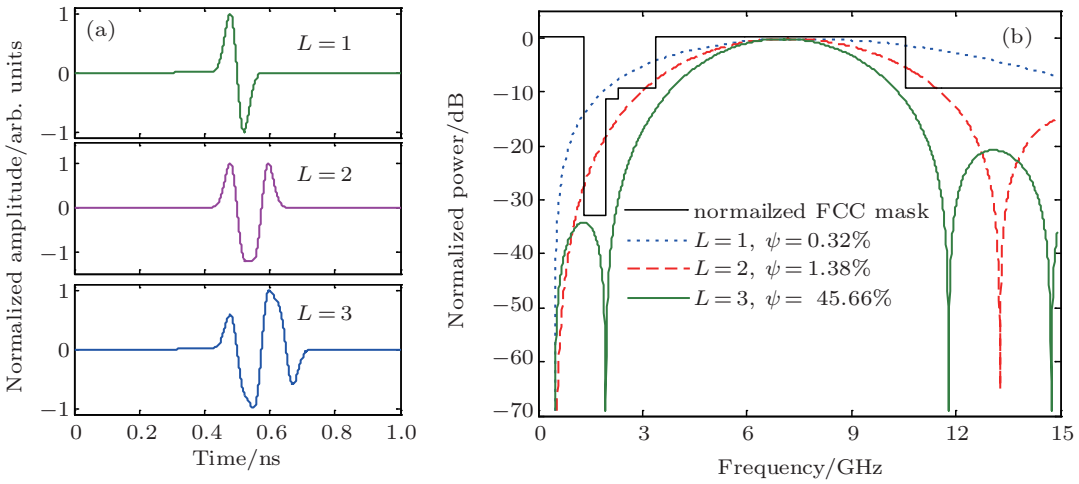


Fig. 2. (colour online) (a) Optimal UWB pulse waveforms and (b) the corresponding spectra for $L = 1$, 2, and 3.

3. Experimental demonstration and discussion

Equation (1) indicates that power-efficient UWB waveforms can be generated by combining three individual monocycle pulses with proper time delays. In our previous work, optical UWB monocycle generation was demonstrated by cross phase modulation (XPM) in an SOA.[5] Inspired by this work, we propose the generation of this power-efficient UWB pulse based on the same principle. The schematic diagram is shown in Fig. 3(a). The Gaussian pulse trains are coupled with three probe signals of continuous wave at different wavelengths, and then launched into a nonlinear SOA simultaneously. All the probe signals have similar phase variations induced by the input Gauss pulse due to the XPM effect. The phase information is converted into the intensity information by three cascaded FBGs. And the output pulses are the first derivatives of the phase information, i.e., monocycle pulses. The spacing between different FBGs is used to align the monocycles with proper delay, thus the designed power-efficient UWB pulse is generated.

Figure 3(b) shows the transmitted spectra of three cascaded FBGs. Since the probe phase varies in proportion to the intensity of the input Gauss pulse approximately, the temporal chirp of probe signal has Gaussian monocycle shape. By locating the probe carriers in the linear scopes (positive/negative) of the transmitted spectra, three monocycle pulses with different polarities are obtained. The weight of each monocycle is determined by the FBG transmission intensity.

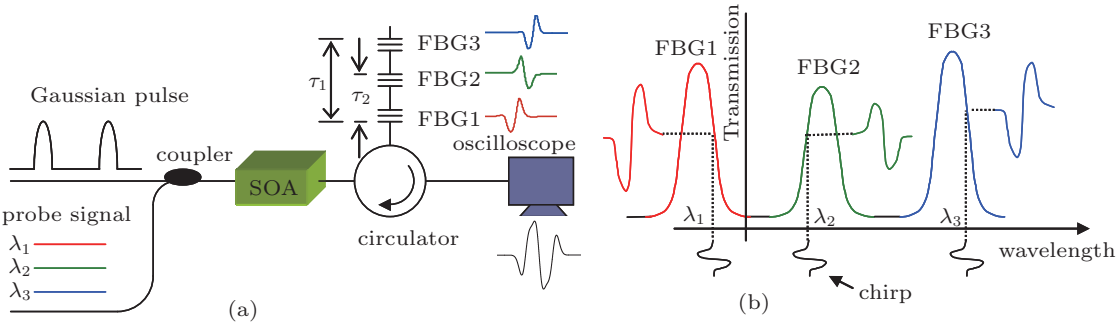


Fig. 3. (colour online) (a) Schematic diagram of generation of power-efficient UWB waveforms based on XPM effect in a single SOA, (b) principle of phase-to-intensity conversion by the FBGs.

In order to prove the feasibility of our scheme, a proof-of-concept experiment is performed as shown in Fig. 4. The first laser diode (LD1) emits an optical Gaussian pulse train, which is generated by a Mach–Zehnder modulator (MZM). The bit rate and pulse width can be controlled by a bit pattern generator (BPG). In our experiment, the Gaussian pulse has a repetition rate of 1.25 GHz, and a pulse width of 50 ps. LD2–LD4 generate another three continuous waves (CW) as probe signals, multiplexed by an arrayed waveguide grating (AWG). Then these four beams are fed to the SOA (CIP nonlinear SOA) for the XPM. All probe signals have similar phase variations to the input Gaussian pulse due to the XPM effect. The SOA is designed for nonlinear optical signal processing with low polarization dependence (< 0.5 dB) and biased 240 mA. Its 1/e gain recovery time is about 25 ps under the operation condition. Since we have no cascaded FBGs in the experiment, alternatively two AWGs are used to filter out three probe beams with proper time delays and then multiplex them into one fiber. Consequently, a fiber delay interferometer (DI) is used to simultaneously convert the phase information into intensity information for the three beams. As such, the probe carriers are located at the linear slopes of the AWG channels respectively. An erbium doped fiber amplifier (EDFA) is used to boost the output optical power. The temporal waveforms, the optical spectra, and the electrical spectra are analysed through a digital communications analyzer (Agilent DCA86100C), an optical spectral analyzer (Anritsu MS9710C), and electrical spectrum analyzer (Anritsu MS2668C), respectively.

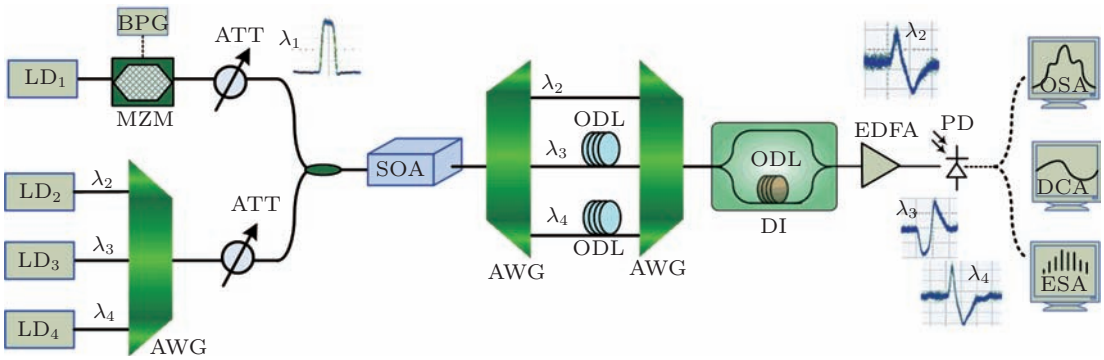


Fig. 4. (colour online) Experimental setup for power-efficient UWB generation, ATT: attenuator, OC: optical coupler, ODL: optical delay line, BPG: bit pattern generator, EDFA: erbium-doped fiber amplifier, PD: photodetector.

Attenuators (ATT) are used to adjust the optical powers of input signals. The wavelength and the peak power of input Gaussian pulses are fixed at 1563.5 nm and 7 dBm, respectively. The fiber DI reveals a comb spectrum, whose frequency shift can be adjusted by a voltage controller. The free spectral range (FSR) of the fiber DI is 40 GHz. By finely tuning the probe wavelength or tuning the spectral shift of the DI, a pair of polarity-reversed monocycle pulses can be achieved, depending on the filtering conditions. The probe power is around 5.2 dBm. When the probe wavelengths are tuned at 1554.15 nm (CH1), 1555.95 nm (CH2), and 1559.60 nm (CH3), three monocycle pulses are obtained respectively, and the temporal waveforms are shown in Fig. 5(b). The DI spectra and corresponding input probe wavelengths

are shown in Fig. 5(a). One can see that the probe carrier of CH1 is located at the DI's positive slope, so is CH3 but opposite is CH2. Therefore, both positive monocycles are generated from CH1 and CH3, but the negative one is obtained from CH2. By properly adjusting the time delay ($T_0 = 55$ ps) between the three monocycles, a combined waveform ($L = 3$) is generated, which is shown as waveform W1 of Fig. 6(a). The pulse width is about 310 ps. The calculated waveforms are plotted as dot lines for comparison. We also measure the corresponding RF spectrum, as shown with S1 of Fig. 6(b). It is shown that most of the RF components are covered by the FCC mask (dash lines), except for a little overflow at 1.25 GHz. When all the probe wavelengths are tuned to the opposite linear slope of the DI spectrum, we obtain a totally opposite UWB waveform, marked as W2. The corresponding RF spectrum is shown as S2 of Fig. 6(b). The normalized RF spectrum is covered mainly by the FCC mask, indicating high power efficiency.

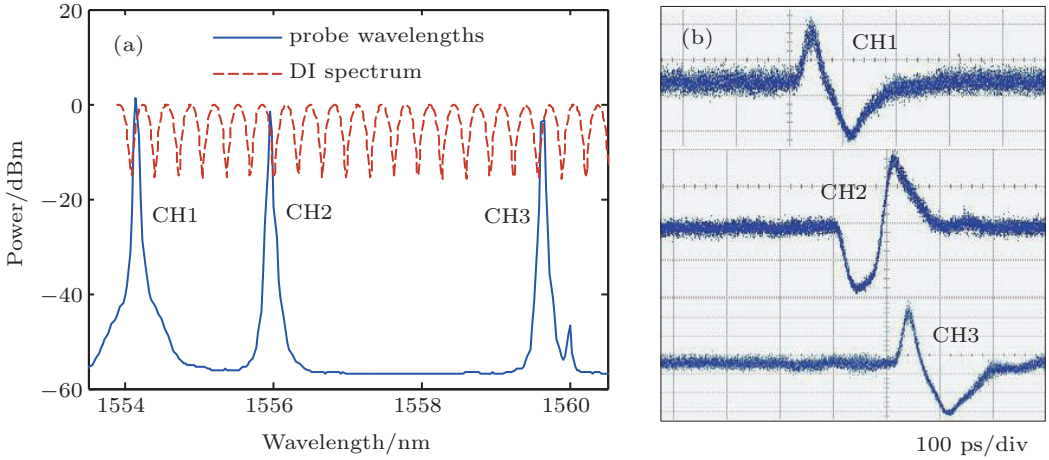


Fig. 5. (colour online) (a) Input probe spectra and the DI spectral response, (b) generated monocycle pulses at the DI output.

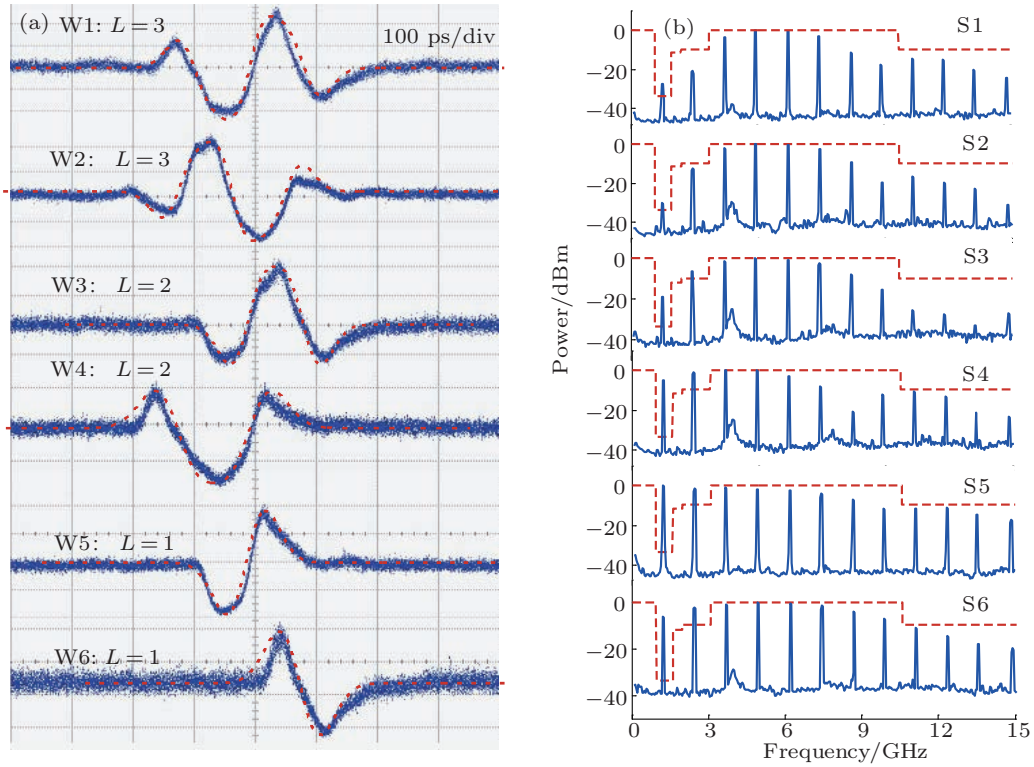


Fig. 6. (colour online) (a) Measured UWB pulse compared with the calculated pulse, W1–W6 are the generated UWB waveforms of $L = 3$, $L = 3$, $L = 2$, $L = 2$, $L = 1$, $L = 1$, respectively. Dot lines denote the calculated pulses correspondingly. (b) Measured RF spectra of generated UWB pulses, where S1∼S6 are corresponding to W1–W6, and the dash lines refer to the FCC spectral mask.

For comparison, we also measure a pair of polarity-reversed designed waveforms with $L = 2$, and $L = 1$ (i.e., monocycle), which are shown as W3–W6 in Fig. 6(a). The dot lines represent the calculated standard waveforms accordingly. Good agreement between the calculated and the measured waveforms is shown. Figure 6(b) shows the measured RF spectra accordingly (S3–S6). Comparing the UWB waveforms of $L = 1$, $L = 2$, and $L = 3$, we can indicate that only RF spectrum of $L = 3$ matches perfectly with the FCC mask, and there are large spectrum overflows for $L = 1$ and $L = 2$. For quantitative analysis, the values of power efficiency ψ are calculated to be low for all the cases (S1–S6), summarized in Table 1. First, the RF spectral envelope is calculated by cubic spine interpolation of discrete frequency components. Then the power efficiency is calculated with Eq. (2). The power efficiency of waveform of $L = 3$ is greatly improved compared with the cases of $L = 2$, and $L = 1$. This proves our previous theoretical calculation. However, the measured power efficiency of $L = 3$ is still not so high as the theoretical value. The main reason lies in that the low frequency component (1.25 GHz) has a little overflow to the FCC mask, and the power efficiency is calculated by attenuating the total power so that all RF components are below the FCC mask.

Table 1. Power efficiencies of UWB RF spectra for $L = 1$, $L = 2$, and $L = 3$.

	$L = 3$		$L = 2$		$L = 1$	
Power efficiency (ψ)	Positive	Negative	Positive	Negative	Positive	Negative
	11.3%	25.9%	2.3%	0.2%	0.08%	0.22%

4. Conclusion

We theoretically proposed an FCC-compliant power-efficient UWB pulse generator by combining three monocycle units with different weights and time delays. And we presented a power-efficient UWB pulse generator based on XPM effect in a single SOA. A proof-of-concept experiment was demonstrated to prove the feasibility of our scheme. The RF spectra of $L = 3$, $L = 2$, and $L = 1$ were compared. It is shown that the power efficiency of $L = 3$ is greatly improved compared with those of $L = 2$ and $L = 1$. Our proposed scheme is very simple, cost effective, and robust in all-optical operation.

References

[1] Aiello G R and Rogerson G D 2003 *IEEE Microw. Mag.* **4** 36

[2] Porcino D and Hirt W 2003 *IEEE Commun. Mag.* **41** 66

[3] Jensen J B, Rodes R, Caballero A, Yu X, Gibbon T B and Monroy I T 2009 *Opt. Express* **17** 16898

[4] Dong J J, Zhang X L and Huang D X 2008 *Chin. Phys.* B **17** 4226

[5] Dong J J, Zhang X L, Fu S N, Shum P and Huang D X 2007 *Chin. Phys. Lett.* **24** 990

[6] Dong J J, Zhang X L, Fu S N, Shum P and Huang D X 2007 *Acta Phys. Sin.* **56** 2250 (in Chinese)

[7] Yao J P 2009 *IEEE Microwave Mag.* **10** 82

[8] Wang Q, Zeng F, Blais S and Yao J P 2006 *Opt. Lett.* **31** 3083

[9] Dong J J, Zhang X L, Zhang Y and Huang D X 2008 *Electron. Lett.* **44** 1083

[10] Zhou E B, Yu X B, Zhang X L, Xue W Q, Yu Y, Mϕrk J and Monroy I T 2009 *Opt. Lett.* **34** 1336

[11] Zheng J Y, Zhang M J, Wang A B and Wang Y C 2010 *Opt. Lett.* **35** 1734

[12] Juan Y S and Lin F Y 2010 *Opt. Express* **18** 9664

[13] Dong J J, Zhang X L, Yu Y, Xu J and Huang D X 2008 *Chin. Phys. Lett.* **25** 911

[14] Li J, Liang Y and Wong K K Y 2009 *IEEE Photon. Technol. Lett.* **21** 1172

[15] Wang Y J, Wu C Q, Xin X J, Yu K L and Zhang X L 2010 *Chin. Phys.* B **19** 094210

[16] Zhou L N, Zhang X L, Xu E M and Huang D X 2009 *Acta Phys. Sin.* **58** 1036 (in Chinese)

[17] Bolea M, Mora J, Ortega B and Capmany J 2010 *Opt. Express* **18** 26259

[18] Yao J P 2010 *Nature Photon.* **4** 79

[19] Abtahi M, Dastmalchi M, LaRochelle S and Rusch L A 2009 *J. Lightwave Technol.* **27** 5276

[20] Abtahi M, Magné J, Mirshafiei M, Rusch L A and LaRochelle S 2008 *J. Lightwave Technol.* **26** 628

[21] Abraha S T, Yang H, Tangdiongga E and Koonen A M J 2009 *International Topical Meeting on Microwave Photonics* 2009 Valencia, Spain p. 1

[22] Zhou E B, Xu X, Liu K S and Wong K K Y 2010 *IEEE Photon. Technol. Lett.* **22** 1063

[23] Dong J J, Zhang Y, Yu Y, Huang D X and Zhang X L 2010 *Asia Communications and Photonics Conference* (ACP), 2010 Shanghai, China p. 693